



Contents lists available at ScienceDirect

Spectrochimica Acta Part A: Molecular and Biomolecular Spectroscopy

journal homepage: www.elsevier.com/locate/saa

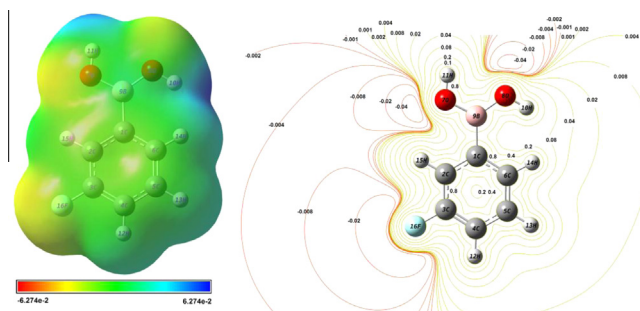
DFT calculations and experimental FT-IR, FT-Raman, NMR, UV-Vis spectral studies of 3-fluorophenylboronic acid

M. Karabacak^a, E. Kose^{b,*}, E.B. Sas^c, M. Kurt^c, A.M. Asiri^{d,e}, A. Atac^b^a Department of Mechatronics Engineering, H.F.T. Technology Faculty, Celal Bayar University, Turgutlu, Manisa, Turkey^b Department of Physics, Celal Bayar University, Manisa, Turkey^c Department of Physics, Ahi Evran University, Kirsehir, Turkey^d Department of Chemistry, Faculty of Science, King Abdulaziz University, Jeddah, Saudi Arabia^e Center of Excellence for Advanced Materials Research, King Abdulaziz University, Jeddah, Saudi Arabia

HIGHLIGHTS

- Monomeric conformations and dimeric structure of 3-fluorophenylboronic acid were investigated.
- The compound was characterized by FT-IR, FT-Raman, NMR and UV spectroscopies.
- The vibrational frequencies, chemical shifts and electronic absorption wavelengths were calculated by DFT.

GRAPHICAL ABSTRACT



ARTICLE INFO

Article history:

Received 10 May 2014

Received in revised form 11 August 2014

Accepted 31 August 2014

Available online 5 October 2014

Keywords:

3-Fluorophenylboronic acid
 FT-IR and FT-Raman spectra
 NMR and UV spectra
 Density of state
 NLO

ABSTRACT

The spectroscopic (FT-IR, FT-Raman, ¹H and ¹³C NMR, UV-Vis), structural, electronic and thermodynamical properties of 3-fluorophenylboronic acid (C₆H₄FB(OH)₂, 3FPBA) were submitted by using both experimental techniques and theoretical methods (quantum chemical calculations) in this work. The experimental infrared and Raman spectra were obtained in the region 4000–400 cm⁻¹ and 3500–10 cm⁻¹, respectively. The equilibrium geometry and vibrational spectra were calculated by using DFT (B3LYP) with 6-311++G(d,p) basis set. The vibrational wavenumbers were also corrected with scale factor to take better results for the calculated data. The total energy distributions (TED) of the vibrational modes were performed for the assignments of the title molecule by using scaled quantum mechanics (SQM) method. The NMR chemical shifts (¹H and ¹³C) were recorded in DMSO solution. The ¹H and ¹³C NMR spectra were computed by using the gauge-invariant atomic orbital (GIAO) method, showing a good agreement with the experimental ones. The last one UV-Vis absorption spectra were analyzed in two solvents (ethanol and water), saved in the range of 200–400 nm. In addition these, HOMO and LUMO energies, the excitation energies, density of states (DOS) diagrams, thermodynamical properties and molecular electrostatic potential surface (MEPs) were presented. Nonlinear optical (NLO) properties and thermodynamic features were performed. The experimental results are combined with the theoretical calculations using DFT calculations to fortification of the paper. At the end of this work, the results were proved our paper had been indispensable for the literature backing.

© 2014 Elsevier B.V. All rights reserved.

* Corresponding author. Tel.: +90 236 2013131.

E-mail address: etemmm43@gmail.com (E. Kose).

Introduction

The organic compounds, containing boron, have found widespread use in synthetic organic chemistry. Boronic acids are not occurring naturally, though they have appeared in the literature since at least 1860 [1]. Unique and versatile reactivity and stability of boronic acids have led to uses in numerous areas, including C–C bond formation, acid catalysis, asymmetric synthesis, carbohydrate analysis, metal-catalysis, molecular sensing, and as therapeutic agents, enzyme inhibitors, and novel materials [2–4]. Also several unique characteristic of boronic acids make them well suited for biomedical applications and they and their wide types of derivatives are far-going many areas [5].

The molecular structures of phenylboronic acid and its derivatives have been studied many authors for years [6–15]. Rettig and Trotter [6] studied crystal and molecular structures of phenylboronic acid. Infrared spectra of phenylboronic acid and diphenyl phenylboronate were presented by Faniran [7]. The molecular structures of phenylboronic acid and its dimer using X-ray structural analysis and spectroscopic methods were published [8]. The crystal structure of 3-fluorophenylboronic acid was identified by Wu et al. [9]. Shimpi et al. [10] reported the crystal structures of 4-chloro- and 4-bromophenylboronic acids and hydrates of 2- and 4-iodophenylboronic acid in two different forms, which were characterized by single-crystal X-ray diffraction method. Rodriguez et al. [11] prepared the crystal structure of 2,4-difluorophenylboronic acid. The molecular and crystal structures of 3-formylphenylboronic acid and 3-aminophenylboronic acid monohydrate were analyzed [12,13].

DFT calculations reported to provide excellent vibrational frequencies of organic compounds if the calculated frequencies are scaled to compensate for the approximate treatment of electron correlation, for basis set deficiencies and for the anharmonicity [16–20]. The experimental and theoretical (DFT) spectroscopic studies of 4-chloro- and 4-bromophenylboronic acids [21], 3,4-dichlorophenylboronic acid [22], 2,4- and 2,6-dimethoxy phenylboronic acids [23,24], 3- and 4-pyridineboronic acid molecules [25] were reported. Sachan et al. [26] studied the theoretical and experimental analysis of 2-thienylboronic acid. Moreover the experimental and theoretical investigation of the conformation, vibrational and electronic transitions of 2,3-difluorophenylboronic acid molecule and acenaphthene-5-boronic acid were published [27,28]. The experimental and theoretical investigation of the conformation, vibrational and electronic transitions of methylboronic acid were set out by Rani et al. [29].

This work is a continuation of our previous studies [14,15,27] and the detailed literature survey showed that to the best of our knowledge neither theoretical (DFT) nor experimental spectroscopic study are performed on the conformation, vibrational IR and Raman NMR and UV–Vis spectra of 3FPBA. The detailed description of the title molecule was established both experimentally (FT-IR and FT-Raman, ^1H and ^{13}C NMR and UV–Vis spectra) and theoretically (DFT). Moreover, the heat capacity, entropy, and enthalpy were investigated of the title molecule based on the changes in the different temperatures. In addition these, HOMO and LUMO energies, the excitation energies, DOS diagrams, and MEPs were presented. Furthermore, NLO (the dipole moment, anisotropy of polarizability and first hyperpolarizability) features of 3FPBA molecule were also computed on theoretical calculations.

Experimental details

The 3FPBA was provided from Across Organics Company in solid state with a stated purity of greater than 97% and no further purification. The FT-IR and FT-Raman spectra of the title molecule were recorded in the region $4000\text{--}400\text{ cm}^{-1}$ and $3500\text{--}10\text{ cm}^{-1}$,

respectively. Perkin–Elmer FT-IR System Spectrum BX spectrometer by using a KBr disc technique, at room temperature, with a scanning speed of $10\text{ cm}^{-1}\text{ min}^{-1}$ and the spectral resolution of 4.0 cm^{-1} was used for FT-IR spectrum. Bruker RFS 100/S FT-Raman instrument using 1064 nm excitation from an Nd:YAG laser was used, the detector is a liquid nitrogen cooled Ge detector, five hundred scans were accumulated at 4 cm^{-1} resolution using a laser power of 100 mW for FT-Raman spectrum. The NMR (^1H and ^{13}C) spectra of the title molecule were carried out in Varian Infinity Plus spectrometer at 300 K , dissolved in DMSO. The chemical shifts were reported in ppm relative to tetramethylsilane (TMS). Lastly the UV–Vis spectra of 3FPBA were registered in the range of $200\text{--}400\text{ nm}$ using Shimadzu UV-2101 PC, UV–VIS recording spectrometer. The 3FPBA molecule was solved in ethanol and water.

Quantum chemical calculations

We have utilized DFT theory for the computation of molecular structure, vibrational frequencies and energies of optimized structures. Because of considerable effort has been directed to the understanding of organic molecule of theoretical calculations with the DFT [30] with the Becke's three-parameter hybrid functional (B3) [31] for the exchange part and the Lee–Yang–Parr (LYP) correlation function [32], accepted as a cost-effective approach. Therefore, geometrical parameters, IR, Raman, (^1H and ^{13}C) NMR and UV–Vis spectra of the heading molecule (in the ground state) were calculated in tandem with Gaussian09 suite of quantum chemical codes [33].

To find the most stable structure of 3FPBA molecule, firstly four possible conformers are proposed as named *Trans–Cis* (TC), *Cis–Trans* (CT), *Trans–Trans* (TT) and *Cis–Cis* (CC) and optimized by using the hybrid B3LYP level of theory in DFT with the 6-311++G(d,p) basis set [31,32]. Then the selected torsion angle is changed every 10° and molecular energy profile is calculated from 0° to 360° for all conformers. The optimized structural parameters were used in the vibrational frequencies, isotropic chemical shifts and calculations of electronic properties. The harmonic frequencies were multiplied by scaled factors to obtain the best agreement results with the experimental data. The scaling factors are used as 0.958 for greater and 0.983 smaller than 1700 cm^{-1} , respectively. [34,35]. The SQM method and PQS program [36,37] were utilized for computations of the TED of fundamental vibrational modes and characterized.

The GIAO method is one of the most common approaches for calculating nuclear magnetic shielding tensors and accurate predictions of molecular geometries are essential for reliable studies of magnetic properties. The GIAO method [38] is used to carry out ^1H and ^{13}C NMR isotropic shielding using the optimized parameters. The time-dependent DFT (TD-DFT) approach is used to obtain the UV–Vis spectrum, electronic transitions, vertical excitation energies, and absorbance wavelengths and oscillator strengths of 3FPBA. GaussSum 2.2 program [39] is run out to analysis group contributions of molecular orbitals and to graphs total density of states (TDOS or DOS), the partial density of states (PDOS) and overlap population density of states (OPDOS) spectra, by convoluting the molecular orbital information with Gaussian curves of unit height and a FWHM (Full Width at Half Maximum) of 0.3 eV .

The MEPs of 3FPBA molecule is represented and evaluated. The heat capacity, entropy, and enthalpy of the title molecule were calculated for the different temperature (from 100 K to 700 K). The dipole moment and NLO properties of 3FPBA molecule were calculated and interpreted.

Results and discussion

The 3FPBA molecule has two substituents such that $\text{B}(\text{OH})_2$ group, (have hydroxyl groups attached to boron) and F (Fluorine)

atom is at *meta*- position. The model system (based on boronic acid (hydroxyl groups) and F atom) are chosen to find the most stable one within four possible conformers/isomers.

Potential energy surface (PES) scan and Energetics

The plausible four conformers of 3FPBA molecule are analyzed, due to the structure of model system boronic acid, dependent on the positions of the hydrogen atoms bonded to oxygen, whether they are directed away from or towards the ring (Fig. 1). Additionally, to explain conformational features of 3FPBA a conformational analysis is performed between phenyl ring and B(OH)₂ group system. To analysis conformational flexibility of 3FPBA, the energy profile of the four (TC/CT conformers have the same scan) proposed conformers as a function of T(O₈–B₉–C₁–C₂), torsion angle was varied from 0° to 360° by changing every 10° by using B3LYP/6-311G++(d,p) method. The conformational analysis show that there is one local minima near 0° (or 180° or 360°) T(O₈–B₉–C₁–C₂) torsion angle for TC/CT and TT conformers. The CC conformer showed that also one local minimal cavity at the near 30° (or 150° or 210° or 330°) given Fig. S1. It is clear that the conformer is more stable for 0° torsion angle (TC conformer) of 3FPBA molecule.

The energies of the different plausible conformers (based on the location of hydrogen atom of the molecule and then scan results) of the headline molecule are optimized DFT/B3LYP/6-311++G(d,p) for C₁ and C_s symmetry point groups. The calculated energies were showed that TC form is more stable conformer than the other conformers. TC, CT, and CC conformers have the negative frequency while TT conformer has positive frequency for C_s symmetry point group. However all conformers have no negative frequency for C₁ symmetry point group. Therefore using the as reference point [the lowest energy (C₁ symmetry point group) (TC)], the relative energy of the other conformers was as: $\Delta E = E(C_n) - E(C_{TC})$. The energies and the energy differences of 3FPBA molecule were determined in Table 1. The energy of TC conformer differs from by value

0.0877 to 3.3371 kcal/mol than the other conformers of the caption molecule for C₁ symmetry point group. The discussion below refers only for the most stable TC conformer. For this reason, the geometric parameters, vibrational frequencies, NMR chemical shifts and UV–Vis absorption spectrum of TC conformer of the title molecule (C₁ symmetry point group) were reported by using 6-311++G(d,p) with the comparing experimental results.

Geometrical structures

The crystal structure of the phenylboronic acid and 3-fluorophenylboronic acid were reported in the literature [6,9]. Therefore the geometric parameters, bond lengths and angles, compared with the structure of phenylboronic acid and 3-fluorophenylboronic acid [6,9].

The four possible structures of 3FPBA molecule, TC [most stable], CT, TT and CC and its atomic numbering schemes are shown in Fig. 1. Also the atomic numbering scheme of TC dimer form of 3FPBA molecule is shown in Fig. 2. The optimized geometry parameters, in accordance with the atom numbers of Fig. 1, (bond lengths and bond angles) of the monomer and dimer structures of TC conformer of the title molecule are given in Table 2. The optimized geometry parameters of four possible conformers of 3FPBA molecule are gathered in Table S1. The theoretical computations are general slightly overestimate bond lengths and angles from the experimental results [6,9]. The discrepancies of the molecular geometry of 3FPBA between gas phase and solid phase, owing to extended hydrogen bonding and stacking interactions, are appropriate.

The C–C bond lengths were observed in the range of 1.365–1.406 Å for 3-fluorophenylboronic acid [9], from 1.378 to 1.404 Å for the phenylboronic acid [6]. These bond lengths are also calculated in the previous for similar molecules like; they are calculated in the range of 1.384–1.407 Å for 2,3-difluorophenylboronic acid [27]. In this study, we calculated the C–C bond lengths in the range of 1.384–1.404 Å by using B3LYP/6-311++G(d,p). The C–H bonds

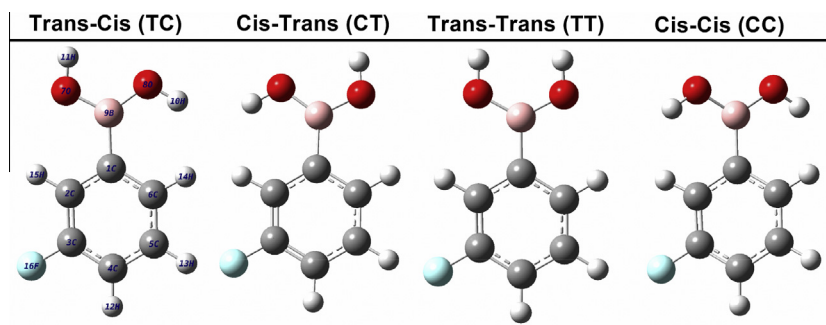


Fig. 1. The monomer theoretical optimized geometric structures of 3FPBA.

Table 1

The calculated energies and energy differences for four possible conformers of 3FPBA by DFT (B3LYP/6-311++G(d,p)) method.

Conformers	Energy		Energy differences ^a		Dipole moment (Debye)	Imaginary frequencies
	(Hartree)	(kcal/mol)	(Hartree)	(kcal/mol)		
<i>C₁</i> symmetry						
Trans–Cis (TC)	–507.66423974	–318564.1332	0.0000	0.0000	2.7815	–
Cis–Trans (CT)	–507.66409991	–318564.0455	0.0001	0.0877	0.5152	–
Trans–Trans (TT)	–507.66118657	–318562.2174	0.0031	1.9159	3.6493	–
Cis–Cis (CC)	–507.65892166	–318560.7961	0.0053	3.3371	2.7449	–
<i>C_s</i> symmetry						
Trans–Cis (TC)	–507.66422543	–318564.1243	0.0000	0.0090	2.7815	–12.70 cm ^{–1}
Cis–Trans (CT)	–507.66407732	–318564.0313	0.0002	0.1019	0.5152	–23.34 cm ^{–1}
Trans–Trans (TT)	–507.66117602	–318562.2107	0.0031	1.9225	3.6493	–
Cis–Cis (CC)	–507.65765690	–318560.0025	0.0066	4.1308	2.7449	–81.27 cm ^{–1}

^a Energies of the other three conformers relative to the most stable TC (for C₁ symmetry point group) conformer.

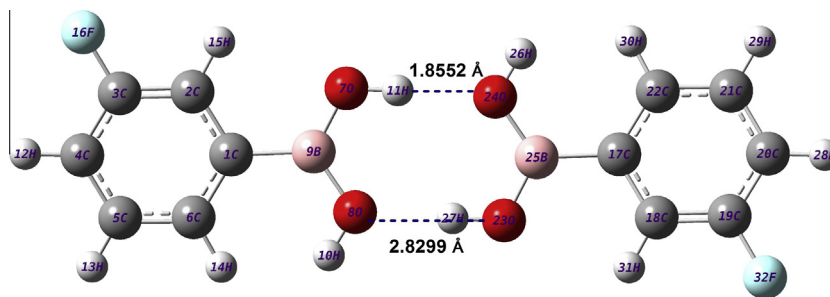


Fig. 2. The dimer theoretical optimized geometric structure of TC conformer of 3FPBA.

lengths for 3FPBA molecule are approximately (except little difference) equal to for the experimental values both of phenylboronic acid and 3-fluorophenylboronic acid [6,9]. The C–C and C–H bond lengths are showed good agreement with aforementioned literature [21–29].

The C–B experimental values of phenylboronic acid and 3-fluorophenylboronic acid are in well coherent, observed at 1.568 Å and 1.562 Å [6,9]. The C–B bond TC (monomer and dimer) and CT form of the C–F bond length is 1.37 studied molecule was calculated at 1.569 Å showed very good correlation with structurally similar molecules in the literature. However this bond computed at 1.563 Å and 1.579 Å form TT and CC form, respectively. The optimized C–B bond length was calculated at 1.575 Å for the 2,3-DFPBA in our previous work [27].

The bond lengths of O–B are observed at 1.362 Å and 1.378 Å for phenylboronic acid [6], at 1.343 Å and 1.366 Å for 3-fluorophenylboronic acid molecule [9]. Also in the previous work, O–B distances including for the different forms were calculated at 1.366 Å and 1.373 Å for 3,4-dichlorophenylboronic acid [22]. These distances were presented from 1.371 Å to 1.375 Å and 1.365 Å to 1.373 Å, for the 2,4- and 2,6-dimethoxyphenylboronic acid molecule, respectively [23,24]. The optimized O–B bond lengths were calculated ca. 1.360 Å and 1.375 Å in previous study [27]. In this work, these bond lengths are calculated at 1.366 Å and 1.373 Å (O₇–B₉ and O₈–B₉) for TC and CT forms of the title molecule, showed coherent with the experimental values and above mentioned the calculation results of the literature. But the O–B bonds were computed at 1.373 Å (O₇–B₉ and O₈–B₉) for TT form and at 1.366 Å (O₇–B₉ and O₈–B₉) for CC form. This can be the state of hydrogen atoms. There is seen decrease O₇–B₉ bond while increase O₈–B₉ for the dimer structure of TC conformer accordance of the monomer. These can be derived from inter and intra-molecular interaction.

The C–X (X; F, Cl, Br ...) bond length shows a remarkable increase when substituted (X) in place of hydrogen atom. In international tables for crystallography, the C–F bond length is 1.377 Å for 3-fluorophenylboronic acid [6]. The C–F bond length was observed and calculated at 1.357 Å for 5-fluoro salicylic acid (similar structure for our molecule) [40,41]. In this work, the bond C–F is calculated at 1.357 Å, by using B3LYP/6-311G++(d,p) basis set, showing good coherent related paper. This bond also was computed the same value for the dimer structure and other conformers.

The ring C–C–C bond angles were observed between 117.6° and 123.9° for 3-fluorophenylboronic acid [9], which is the good correlation (except one or two) with the normal values (120.0°) of the six-membered phenyl ring. However the C₂–C₃–C₄, C₄–C₅–C₆ and C₁–C₆–C₅ bond angles of TC conformer deviated from normal value greater than others, it can be attached fluorine atom and B(OH)₂ group. This deviation also showed the dimer structure of TC conformer and the other conformers. The C–B–O and O–B–O bond angles of the molecule were disparity in the TT and CC conformers from the TC and CT conformers. The hydrogen atoms (attached

Table 2

The optimized geometrical parameters (bond lengths (Å) and angles (°) and experimental of 3FPBA for the monomer and dimer structures of TC conformer.

Parameters	B3LYP/6-311++G(d,p)			
	X-ray ^{a,b}		Monomer	Dimer
Bond Lengths (Å)				
C1–C2	1.404	1.406	1.404	1.404
C1–C6	1.402	1.398	1.404	1.404
C1–B9	1.568	1.562	1.569	1.569
C2–C3	1.389	1.377	1.384	1.383
C2–H15	–	0.930	1.083	1.083
C3–C4	1.378	1.365	1.387	1.387
C3–F16	–	1.377	1.357	1.357
C4–C5	1.384	1.375	1.393	1.393
C4–H12	1.000	0.930	1.083	1.083
C5–C6	1.390	1.387	1.393	1.393
C5–H13	1.000	0.930	1.084	1.084
C6–H14	1.000	0.930	1.086	1.087
O7–B9	1.378	1.343	1.366	1.351
O7–H11	0.750	0.851	0.963	0.975
O8–B9	1.362	1.366	1.373	1.392
O8–H10	0.750	0.855	0.960	0.961
Bond Angles (°)				
C2–C1–C6	117.2	117.6	118.1	118.1
C2–C1–B9	120.8	120.1	119.3	118.8
C6–C1–B9	122.0	122.1	122.6	123.1
C1–C2–C3	121.8	118.6	119.6	119.6
C1–C2–H15	–	120.7	120.7	120.6
C3–C2–H15	–	120.7	119.7	119.8
C2–C3–C4	119.5	123.9	122.6	122.6
C2–C3–F16	–	118.0	118.9	118.9
C4–C3–F16	–	118.1	118.5	118.5
C3–C4–C5	120.3	118.4	118.2	118.2
C3–C4–H12	120.0	120.8	119.9	119.9
C5–C4–H12	120.0	120.8	121.9	121.9
C4–C5–C6	120.1	119.7	120.2	120.2
C4–C5–H13	120.0	120.2	119.6	119.6
C6–C5–H13	120.0	120.2	120.3	120.3
C1–C6–C5	121.1	121.8	121.4	121.4
C1–C6–H14	120.0	119.1	120.5	120.6
C5–C6–H14	120.0	119.1	118.1	118.0
B9–O7–H11	111.0	116.0	112.6	115.1
B9–O8–H10	111.0	124.0	115.1	114.6
C1–B9–O7	118.7	119.0	118.3	119.5
C1–B9–O8	125.0	122.7	124.3	122.3
O7–B9–O8	116.3	118.2	117.4	118.2

^{a,b} The X-ray data from Ref. [6,9].

oxygen atoms) have important role for these disparity. The hydrogen atoms have *trans*–*cis* or *cis*–*trans* orientation for TC and CT conformers. But the hydrogen atoms of the other two conformers are the same orientation (see Table S1). If one see all calculated bond angles; there are some small difference between the calculated and experimental values. This can be due to calculation belongs to gas phase and the experimental result belong to solid phase. One can quite easily see from Table 2, all calculations of the bond angles are in very consistency with the compared experimental values [6,9].

Vibrational spectral analysis

The purpose of this part is to obtain the spectroscopic signature of the title molecule and the assignment of the vibrational absorptions to make a comparison with the results obtained from the theoretical calculations and the structurally similar molecules. The theoretical vibrational analysis were performed by using DFT/B3LYP/6-311G++(d,p) basis set. The calculated wavenumbers usually higher than the experimental ones; this dissimilarity can be a consequence of the anharmonicity and the general tendency of the quantum chemical methods to overestimate the force constants at the exact equilibrium geometry. Also the other possibility is the calculations have been made for free molecules in vacuum, while experiments were performed for solid sample. This discrepancy partly fixed with the scaling factor [34,35]. The experimental and theoretical (with the scaling factor) infrared and Raman spectra are given in Figs. 3 and 4 for comparative purpose, where the calculated intensity is plotted against harmonic vibrational wavenumbers.

The 3FPBA molecule, which has C_1 symmetry, has 16 atoms and 42 fundamental vibrational modes. The optimized molecular conformation exhibits no special symmetries and consequently all the 42 fundamental vibrations of the molecule are both IR- and Raman-active. The calculated wavenumbers of the most stable conformer (*trans-cis*) and the dimer structure of the present molecule were tabulated in Table 3 together with the experimental wavenumbers. A detailed description of the normal modes are performed at the B3LYP level with the triple split valence basis set 6-311++G(d,p), on the basis of relative intensities, line shape and TED given in Table 3. The interpretations include the ring vibrational modes and between the ring and substituent modes. We discussed the vibrational modes under two subhead as $B(OH)_2$ vibrations and phenyl ring vibrations.

$B(OH)_2$ vibrations

The assignment of the O–H stretching vibrations is pure and intelligible. This band absorbs broadly near $3300\text{--}3200\text{ cm}^{-1}$ in boronic acids. It is extremely sensitive to formation of hydrogen bonding. In the spectrum of phenylboronic acid (3280 cm^{-1} in IR) [7], 2,4- and 2,6-dimethoxyphenylboronic acid ($3480, 3339\text{ cm}^{-1}$ in FT-IR) (3335 cm^{-1} in FT-IR and 3278 cm^{-1} in FT-Raman) [23,24] was assigned, which is typical for O–H bonded hydroxyl

groups. In the prior work [27], we recorded this band at 3400 and 3332 cm^{-1} in FT-IR spectrum and predicted value at 3685 ($O_7\text{--}H_{11}$) and 3692 cm^{-1} ($O_8\text{--}H_{10}$) for 2,3-difluorophenylboronic acid. The O–H stretching modes for 2,3-difluorophenylboronic acid were also calculated at 3609 and 3339 cm^{-1} as expected pure stretching modes accordance TED contributing 100%. This frequency is observed at 3244 cm^{-1} in FT-IR for structurally similar molecule [41]. The O–H peaks were observed at 3392 and 3257 cm^{-1} in FT-IR spectrum for acenaphthene-5-boronic acid [28]. In this study, the O–H peak is not observed experimentally but predicted at 3722 cm^{-1} ($O_8\text{--}H_{10}$) and 3686 cm^{-1} ($O_7\text{--}H_{11}$) for monomer structure. Also these band were computed at $3709, 3709\text{ cm}^{-1}$ ($O_8\text{--}H_{10}$) and $3471, 3442$ ($O_7\text{--}H_{11}$) for the dimer structure of the TC form of the title molecule. We can say; due to the inter-molecular effect the $O_7\text{--}H_{11}$ mode was showed downshift effect.

The ν_{19} and ν_{21} modes are assigned as O–H in-plane bending and predicted at 1005 (1004 cm^{-1} in FT-Raman), and 971 cm^{-1} for the monomer structure of TC form of the title molecule. The O–H out-of-plane bending (ν_{27}, ν_{30} and ν_{34}) are computed at $700, 571$ and 461 cm^{-1} for the monomer structure of TC conformer of 3FPBA molecule. This band at 724 and 588 cm^{-1} in FT-Raman and at 722 and 584 cm^{-1} in FT-IR bands is assigned out-of-plane bending while O–H in-plane bending vibration is only recorded in FT-Raman experimentally. We can see in the dimer structure that the O–H bending modes especially in-plane bending modes are increasing due to the inter- and intra-molecular interactions. Theoretical values of O–H bending vibrations are good coherent in experimental values and in the literature [21–29,42,43].

The B–O band is very intense and should also include the asymmetric and symmetric stretching vibrations which are located between 1300 and 1375 cm^{-1} in infrared spectrum for phenylboronic acid and the phenylboronic acid [7,43]. In this study, the calculated B–O stretching modes are assigned at 1366 and 1338 cm^{-1} as asymmetric and symmetric modes, by using B3LYP method for the monomer structure of TC conformer, respectively. The B–O symmetric stretching band is observed at 1340 cm^{-1} in FT-IR and 1341 cm^{-1} in FT-Raman. The TED calculations showed that the B–O asymmetric stretching modes are more clearly a pure mode than the B–O symmetric stretching modes for the monomer structure of TC conformer (Table 3). These modes were showed dissimilarity in the dimer form. It can be the role of hydrogen atoms

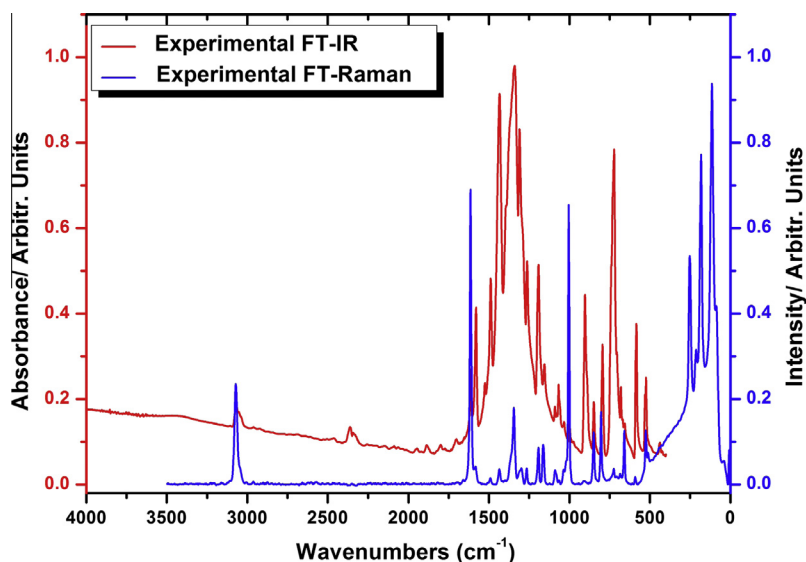


Fig. 3. The experimental FT-IR and FT-Raman spectra of 3FPBA.

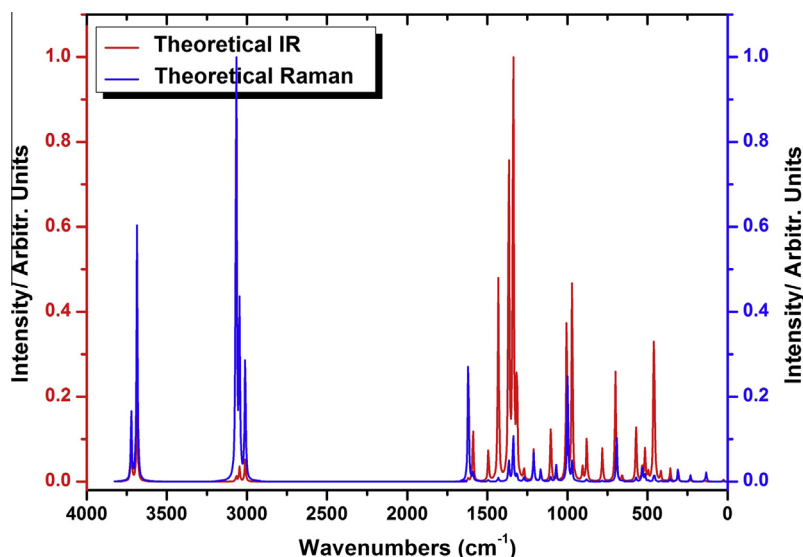


Fig. 4. The calculated infrared and Raman spectra of 3FPBA.

Table 3

The comparison of the calculated harmonic frequencies and experimental (FT-IR and FT-Raman) wavenumbers (cm^{-1}) by using B3LYP method 6-311++G(d,p) basis set for monomer and dimer structures of TC conformer of 3FPBA.

Modes No	Theoretical/monomer		Theoretical/dimer		Experimental		TED ^b ($\geq 10\%$) Monomer
	Unscaled freq.	Scaled freq. ^a	Unscaled freq.	Scaled freq. ^a	FT-IR	FT-Raman	
v1	3885	3722	3872, 3872	3709, 3709			vOH (100) (O ₈ -H ₁₀)
v2	3848	3686	3623, 3593	3471, 3442			vOH (100) (O ₇ -H ₁₁)
v3	3202	3067	3202, 3202	3068, 3068	3069	3070	vCHsym. (99)
v4	3201	3067	3201, 3201	3067, 3067			vCHsym. (99)
v5	3180	3046	3180, 3180	3046, 3046			vCHasym. (100)
v6	3143	3011	3137, 3137	3005, 3005			vCHasym. (100)
v7	1647	1619	1647, 1647	1619, 1619	2364		Overtone + combination
v8	1617	1589	1616, 1616	1589, 1589	1612	1615	vCC (68), δ CCH (12)
v9	1520	1494	1520, 1520	1494, 1494	1580	1493	vCC (65), δ CCH (15)
v10	1456	1431	1458, 1452	1433, 1427	1489		δ CCH (50), vCC (29)
v11	1390	1366	1428, 1425	1404, 1401	1434	1432	vCC (35), δ CCH (25)
v12	1361	1338	1355, 1346	1332, 1323			vBO ₂ asym. (62)
v13	1338	1316	1338, 1319	1315, 1297	1340	1341	vBO ₂ sym. (33), vCB (20), δ CCH (13), vCC (11), δ OH (10)
v14	1293	1271	1293, 1292	1271, 1270	1310	1303	vCC (50), δ CCH (40)
v15	1232	1211	1241, 1238	1220, 1217	1263	1269	δ CCH (43), vCC (41)
v16	1187	1167	1196, 1188	1176, 1168	1192	1191	vCF (37), vCC (18), δ CCH (16)
v17	1123	1104	1147, 1121	1128, 1102	1155	1160	δ CCH (69), vCC (17)
v18	1089	1070	1087, 1068	1069, 1050	1090	1088	δ CCH (39), vCC (33)
v19	1023	1005	1177, 1103	1157, 1084	1067		vCC (37), δ CCH (32)
v20	1016	999	1016, 1015	999, 998		1004	δ OH (78), vBO ₂ sym. (18)
v21	988	971	1020, 1005	1003, 988	1000		vCC (41), δ CCC (39)
v22	968	951	970, 970	954, 954			δ OH (66), vBO ₂ sym. (18)
v23	921	905	923, 923	907, 907	903		γ CH (81) [τ CHCH (56), τ CCCH(25)]
v24	900	885	902, 902	887, 887			γ CH (71) [τ CCCH (26), τ CFCH (25), τ CBCH (20)]
v25	895	879	892, 891	877, 876	848	852	γ CH (88) [τ CCCH (40), τ CHCH(22), τ CBCH (15), τ CFCH (11)]
v26	796	782	797, 797	783, 783	794	806	vCF (24), vCC (21), vBO (15), δ CCC (10)
v27	712	700	713, 711	701, 699	722	724	γ CH (79) [τ CCCH (52), τ CBCH(14), τ CFCH (13)]
v28	705	693	712, 706	700, 694	680	684	γ OH (47), γ CH (30)
v29	670	658	665, 665	654, 654		658	δ CCC (34), vCC (26), vCB (12), δ CCH (12)
v30	581	571	794, 747	751, 734	584	588	τ CCCC (38), τ CCCH (20), γ OH asym. (15)
v31	542	533	590, 553	580, 544			γ OH asym. (73) [τ BOOH (43), τ CBOH(30)]
v32	525	516	535, 532	526, 523	520	522	δ OBO (15), δ CBO (10), δ CCC (25)
v33	505	496	523, 523	514, 514			δ CCC (37), δ OBO (15)
v34	469	461	457, 444	449, 436			τ CCCC (21), τ CBOH (20), τ CCCH (19), τ CCCF (10)
v35	463	456	472, 467	464, 459	437		γ OHasym.(68) [τ BOOH (35), τ CBOH(33)], δ CCF (10)
v36	424	417	429, 426	422, 419			δ CCF (30), δ CCB (14), δ CBO (14), τ BOOH (10), τ CBOH(10)
v37	364	358	381, 374	375, 368			τ CCCC (39), τ CCCH (22), γ OH (22) [τ CBOH (12), τ CCBO (10)]
v38	315	310	345, 328	339, 322			δ CBO (36), δ CCF (29)
v39	236	232	237, 237	233, 233		250	δ BOO (23), vCB (23), δ CBO (19)
v40	149	146	192, 189	189, 186		180	γ CF (68), τ CFCH (16)
v41	136	134	144, 141	142, 139		114	Γ BOOH (89) [δ CCB (63), δ CBO (26)]
v42	26	25	48, 30	47, 29			τ CCCB (45), τ CBCH (18), τ CCBO (15)
							τ CCBO (97)

^a Wavenumbers in the ranges from 4000 to 1700 cm^{-1} and lower than 1700 cm^{-1} are scaled with 0.958 and 0.983 for B3LYP/6-311++G(d,p) basis set, respectively.

^b v; stretching, γ ; out-of plane bending, δ ; in-plane-bending, τ ; torsion, Γ ; rocking.

(attached the oxygen atoms) in the interactions of intra- and inter-molecular. We can also conclude the computed B–O vibrations are good agreement with the experimental values. The band was assigned around at 1370 cm^{-1} as the B–O stretching vibrations for the homo- and hetero tri-nuclear boron complexes by Vargas et al. [44]. The B–O stretching vibrations were observed at 1352 and $1351, 1389\text{ cm}^{-1}$ in FT-IR and FT-Raman and calculated at 1345, 1371 and 1002 cm^{-1} by using B3LYP method assigned as two symmetric and asymmetric modes for derivative of the phenyl boronic acid [27].

The stretching mode between the ring and B(OH)_2 group (C–B stretching) evaluate for ring derivatives of boronic acids. The C–B stretching modes are calculated at 1338, 693 and 310 cm^{-1} by using B3LYP/6-311++G(d,p) in this work. The C–B stretching modes were observed at 1340 and 680 cm^{-1} in FT-IR and 1341, 684 cm^{-1} in FT-Raman for the title molecule. The bands were assigned at 1089 and 1085 cm^{-1} in the spectrum of the normal and deuterated phenylboronic acids, respectively, and at 1084 cm^{-1} in diphenyl phenylboronate as the C–B stretching modes by Faniran and Shurvell [7]. Erdogdu et al. [45] observed at 1354, 708 cm^{-1} in FT-IR and 701 cm^{-1} in FT-Raman for 2-fluorophenylboronic acid. The calculated C–B stretching modes were computed at 1345, 899, 635 cm^{-1} for 2,3 difluorophenylboronic acid, observed at 1352 and 1351 cm^{-1} as the bands in FT-IR and FT-Raman, respectively [27].

The B–O–H bending and torsion modes with the ring and boronic acid groups (except for identified as O–H/C–H in plane and out-of-plane) are separated and mixed the other modes assigned by their TED if any one see pursuit in Table 3. However if one compare the monomer and dimer structures of the title molecule, the O–H or related the interaction modes are different with the each other. The inter- or intra-molecular interactions are important for these type molecules.

Phenyl ring vibrations

The multiple peaks seem in the $3000\text{--}3100\text{ cm}^{-1}$ range which is the characteristic region for the C–H stretching vibrations [46]. In this study, the C–H stretching modes are calculated in the range of $3011\text{--}3067\text{ cm}^{-1}$ for monomer and $3005\text{--}3068\text{ cm}^{-1}$ for dimer structure by using the B3LYP/6-311++G(d,p) method and observed at 3069 and 3070 cm^{-1} in FT-IR and FT-Raman, respectively. The C–H stretching modes are very pure according to TED contribution (ca. 100%). These modes discussed in the literature predicted in the range of $3030\text{--}3150\text{ cm}^{-1}$ for the structurally similar compounds [19,21,22,27,45].

The C–C stretching modes are very much important for the aromatic ring and also highly characteristic. Varsanyi [47] gave that the bands were of variable intensity and have been observed at 1625–1590, 1590–1575, 1540–1470, 1465–1430 and $1380\text{--}1280\text{ cm}^{-1}$ from the frequency ranges for the five bands in the region. The assignments of five bands in IR spectrum of C–C stretching vibrations of phenylboronic acid were assigned in the range of $1620\text{--}1320\text{ cm}^{-1}$ [7]. In this study, the C–C stretching modes are calculated in the region 1619–1431, 1338–1070, and at 999, 879, 693 cm^{-1} for monomer TC conformer of the title molecule. These modes are observed in the range of 1612–1434, 1340–1067, and at 1000, 848, 680 cm^{-1} in FT-IR spectrum and 1615–1432, 1341–1088, 852, 684 cm^{-1} in FT-Raman spectrum in the studied molecule. The highest contributions of C–C stretching vibrations are calculated at 1619 and 1589 cm^{-1} , appeared nearly pure modes with the TED contribution %68 and %65 for monomer structure. The modes of dimer structure were the same parallel except some small deviations. Similarly, the C–C stretching modes were recorded in the range of 1617–1034 cm^{-1} (IR) for 2-fluorophenylboronic acid [45], 1590–1010 cm^{-1} and 1588–1004 cm^{-1} in FT-IR and FT-Raman for 4-bromophenylboronic acid, 1596–1060 cm^{-1} and 1588–1085 cm^{-1} in FT-IR and FT-Raman for

4-chlorophenylboronic acid, respectively [21]. Also they were observed at 1628, 1266, 1214, 1154 cm^{-1} in FT-IR and at 1626, 1590, 1474, 1292, 1269, 1215, 1148 and 1065 cm^{-1} in FT-Raman for 2,3-difluorophenylboronic acid [27]. These modes were supported DFT calculations, computed between 1650 and 990 cm^{-1} by using B3LYP calculations [19,21,22,27,45].

The bending C–H vibrations are recorded in the range of $1000\text{--}1300\text{ cm}^{-1}$ and $750\text{--}1000\text{ cm}^{-1}$ assigned in plane and out-of-plane, respectively [46]. The C–H in-plane bending vibrations are calculated very wide range nearly in the range of carbon–carbon stretching. Namely, the C–H in-plane modes are generally coupled the C–C stretching modes. The C–H out of plane bending modes were assigned ν_{22-24} , and ν_{26} predicted at 951, 905, 885 and 782 cm^{-1} , respectively. The out of plane bending modes are observed at 903, 794 cm^{-1} in FT-IR and at 806 cm^{-1} (FT-Raman), respectively.

The theoretical wavenumbers of C–F stretching vibrations both monomer and dimer structures of the title molecule contaminated with other vibrations especially ring modes; therefore, there is no pure C–F band vibration according to TED results. There is no disparity between the monomer and dimer structures of the molecule. Normally, the C–F stretching modes are very strong in IR spectrum and appear in the range of $1000\text{--}1300\text{ cm}^{-1}$ [48]. The substituted fluorine derivatives were assigned at 1250 cm^{-1} (IR spectrum) as C–F stretching mode by Narasimham et al. [49] and observed in the region $1250\text{--}1350\text{ cm}^{-1}$ [50]. In this study, we recorded at 1192, 848 cm^{-1} and 1191, 852 cm^{-1} in FT-IR and FT-Raman spectra as CF mode. The theoretically calculated modes were at 1211 and 879 cm^{-1} (for monomer structure) 1220, 1217 and 877, 876 cm^{-1} (for dimer structure) by using B3LYP/6-311++G(d,p) basis set, showing well agreement with the literature and experimental results.

The bending C–F modes were predicted at 574, 475, 353, 312, 299 cm^{-1} for C–F in-plane bending modes and 291 and 204 cm^{-1} for C–F out-of-plane bending modes by Karabacak et al. [27]. Erdogdu et al. [45] observed one band at 520 cm^{-1} both in FT-IR and in FT-Raman spectra for 2-fluorophenylboronic acid molecule. According to TED results, the computed values are 461, 456, 358 cm^{-1} for C–F in-plane bending modes (437 cm^{-1} in FT-IR) and at 232 cm^{-1} (250 cm^{-1} in FT-Raman) for C–F out-of-plane bending mode for the monomer structure. The remainder bending and torsion modes of the related fluorine atom accounted in Table 3.

The ring deformation, torsion and C–C–C bending modes fixed with other modes and sometimes missing in FT-IR and FT-Raman spectra. The maximum contribution C–C–C bending mode (ν_{20}) were observed at 1000 cm^{-1} FT-IR, the other (ν_{32}) at 522 cm^{-1} in FT-Raman and 520 cm^{-1} in FT-IR, calculated wavenumbers of these modes coincide at 999 and 516 cm^{-1} (monomer) and at 999, 998 and 526, 523 cm^{-1} (dimer) after scaling. The ring deformation, torsion modes are obtained in a large region and contaminated other modes and also identified as out-of-plane modes of C–H or O–H. Therefore, these modes will not be discussed here. Also the TEDs of these vibrations were aggregated and evaluated this part.

To see correlation between the experimental and calculated wavenumbers were plotted correlation graphics and given in Fig. 5. Also to see the correlations of infrared and Raman were graphed one by one as Fig. S2(a)–(b). The relations between experimental and calculated wavenumbers are usually linear and described for total and one by one as infrared and Raman, respectively by the following equations:

$$v_{\text{cal.}} = 1.0041v_{\text{exp.}} - 2.7859 \quad (\text{Total} - R^2 = 0.9995)$$

$$v_{\text{cal.}} = 0.9991v_{\text{exp.}} + 5.7457 \quad (\text{Infrared} - R^2 = 0.9995)$$

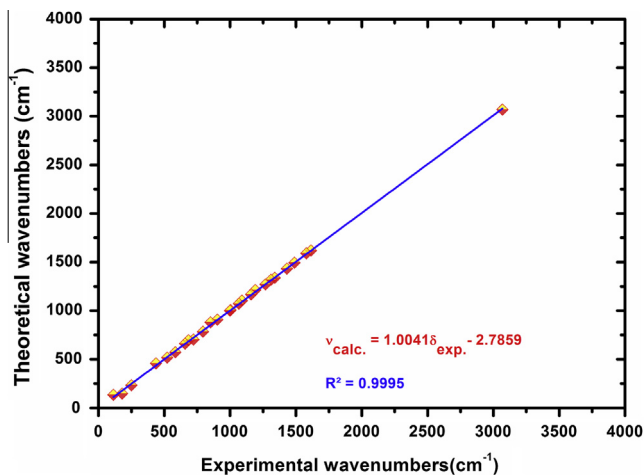


Fig. 5. Correlation graphic of the calculated and experimental frequencies of 3FPBA.

$$v_{\text{cal.}} = 1.0110v_{\text{exp.}} - 7.1223 \quad (\text{Raman} - R^2 = 0.9985)$$

NMR spectrum

The NMR spectroscopy is one of the most important techniques for the structural analysis for organic compounds. It is well-known that the combined use of NMR spectroscopic technique and computer simulation methods offers a powerful way to interpret and predict the even structure of large biomolecules [51]. We also used this technique (^1H and ^{13}C NMR) due to the useful, common and to have more information about the studied molecule. ^1H and ^{13}C NMR analysis of 3FPBA molecule were studied both experimentally and theoretically. The experimental NMR spectra of the headline molecule were given in Fig. 6(a) and (b), respectively. The experimental and theoretical ^1H and ^{13}C chemical shifts in DMSO solvent for monomer and dimer structures were presented in Table 4. The atom positions are listed according to Fig. 1.

To have theoretical NMR results of the title molecule both monomer and dimer structures, the first one; the full geometry optimization of 3FPBA is carried out with the DFT/B3LYP/6-311G++(d,p) basis set. After optimization, ^1H and ^{13}C NMR calculations of the studied compound is calculated by using GIAO [38] and 6-311++G(d,p) basis set IEFPCM/DMSO solvent. Because of GIAO approach to molecular systems was substantially evolved by an efficient application method of ab initio SCF calculations, by using techniques taken from analytic derivative methodologies [38].

There are six hydrogen atoms attached ring and $\text{B}(\text{OH})_2$ group in 3FPBA molecule. The chemical shifts of aromatic protons of organic molecules are usually observed in the region 8.00–7.00 ppm. Because of the electronic environment of the proton, these chemical shifts can change. Electron-withdrawing atom or group (hydrogen attached or nearby) can decrease the shielding and move the resonance of attached proton towards to a higher frequency, while electron-donating atom or group increases the shielding and moves the resonance towards to a lower frequency [52,53]. The proton chemical shifts in the ring are calculated in the range of 7.78–7.24 ppm and 7.95–7.45 ppm for monomer and dimer structures, respectively. The dimer chemical shifts values of H_{14} and H_{15} greater than monomer structure, due to the changed the electronic environment. The experimental values were recorded in the region parts as 7.73–7.75, 7.55–7.67, 7.40–7.47 and 7.18–7.24 ppm. The chemical shift of H_{14} and H_{15} are higher than the other protons. The electronic charge density around of these atoms can be effected the influence of rapid proton exchange, hydrogen bond, solvent effect, etc. in the molecular system. The proton chemical

shifts of H_{10} and H_{11} atoms were not observed experimentally, because of the above reason.

There are also six carbon atoms (in the aromatic ring) in the title molecule. The aromatic carbons give resonances in overlapped areas of the NMR spectrum with chemical shift values from 100 to 150 ppm [54,55]. The calculated and experimental ^{13}C NMR chemical shifts of the present molecule were showed the same parallel with this range and good coherent with the each other. The chemical shifts of the carbon atoms of 3FPBA are calculated at 174.13, 134.94, 133.36, 131.01, 127.11, and 123.82 ppm (monomer) and also at 171.65, 134.84, 133.00, 137.90, 125.70 and 123.39 ppm (dimer). These chemical shifts are recorded at 162.64, 141.87, 130.07, 129.80, 119.65 and 116.77 ppm, respectively. The C_4 atom has smaller chemical shifts (both experimental and theoretical) than the other ring carbon atoms, due to shielding effect which the non-electronegative property of $\text{B}(\text{OH})_2$ group. The value of C_3 atom has the biggest one, because of the electronegative feature of the fluorine atom, the carbon atom (C_3) resonance at lower field, and the signal of this carbon atom is recorded at 162.64 and calculated at 174.13 ppm for monomer, at 171.65 ppm for dimer structure of the title molecule. Moreover, taking a glance at the literature the results of chemical shift of the molecule were showed very good correlation for the structurally similar molecules [27–29].

The correlation graphic is given as Fig. 7 between the experimental and calculated chemical shifts of the title molecule. The average values are used for the correlation graph of ^1H chemical shifts. The correlation graphics (^1H and ^{13}C NMR) are presented in Figs. S3 and S4, respectively. The following equations are given to see the relations between the experimental and calculated chemical shifts:

$$\text{Total} : \delta_{\text{cal}} (\text{ppm}) = 1.0309 \delta_{\text{exp}} - 0.1988 \quad (R^2 = 0.9952)$$

$$^1\text{H} : \delta_{\text{cal}} (\text{ppm}) = 0.9916 \delta_{\text{exp}} + 0.0893 \quad (R^2 = 0.9952)$$

$$^{13}\text{C} : \delta_{\text{cal}} (\text{ppm}) = 1.0287 \delta_{\text{exp}} + 0.1016 \quad (R^2 = 0.8802)$$

The ^1H NMR calculations gave a slightly better coefficient and lower standard error ($R^2 = 0.9952$) than for ^{13}C ($R^2 = 0.8802$) chemical shifts. Based on the ^1H and ^{13}C chemical shifts data of both monomer and dimer structures collected in Table 4. One can deduce that qualitatively the ^1H and ^{13}C NMR chemical shifts of the 3FPBA are described fairly well. However, the small deviation between the experimental and computed chemical shifts of these protons may be due to the presence of intermolecular hydrogen bonding also the solvent effects.

Electronic properties

UV-Vis spectrum and frontier molecular orbital analysis

The TD-DFT calculations to predict the electronic absorption spectrum are a quite reasonable method. TD-DFT methods are computationally more expensive than semi-empirical methods but allow easily studies of medium size molecules [56,57]. Because of this, the TD-DFT calculations with the B3LYP/6-311++G(d,p) method were preferred for UV-Vis spectra and electronic properties theoretically for monomer and dimer structures of the most stable conformer. Also the UV-Vis (electronic absorption) spectra of 3FPBA molecule are recorded in ethanol and water at room temperature. The experimental and theoretical UV-Vis spectra of the studied molecule are shown in Fig. 8. The experimentally absorption values are 268.87, 217.21 nm (in ethanol) and 269.72, 216.13 nm (in water). The calculated values are 248.21, 219.67 and 202.75 nm (in ethanol), 248.12, 219.54 and 202.40 nm (in water) with B3LYP/6-311++G(d,p) basis set. However the calculated

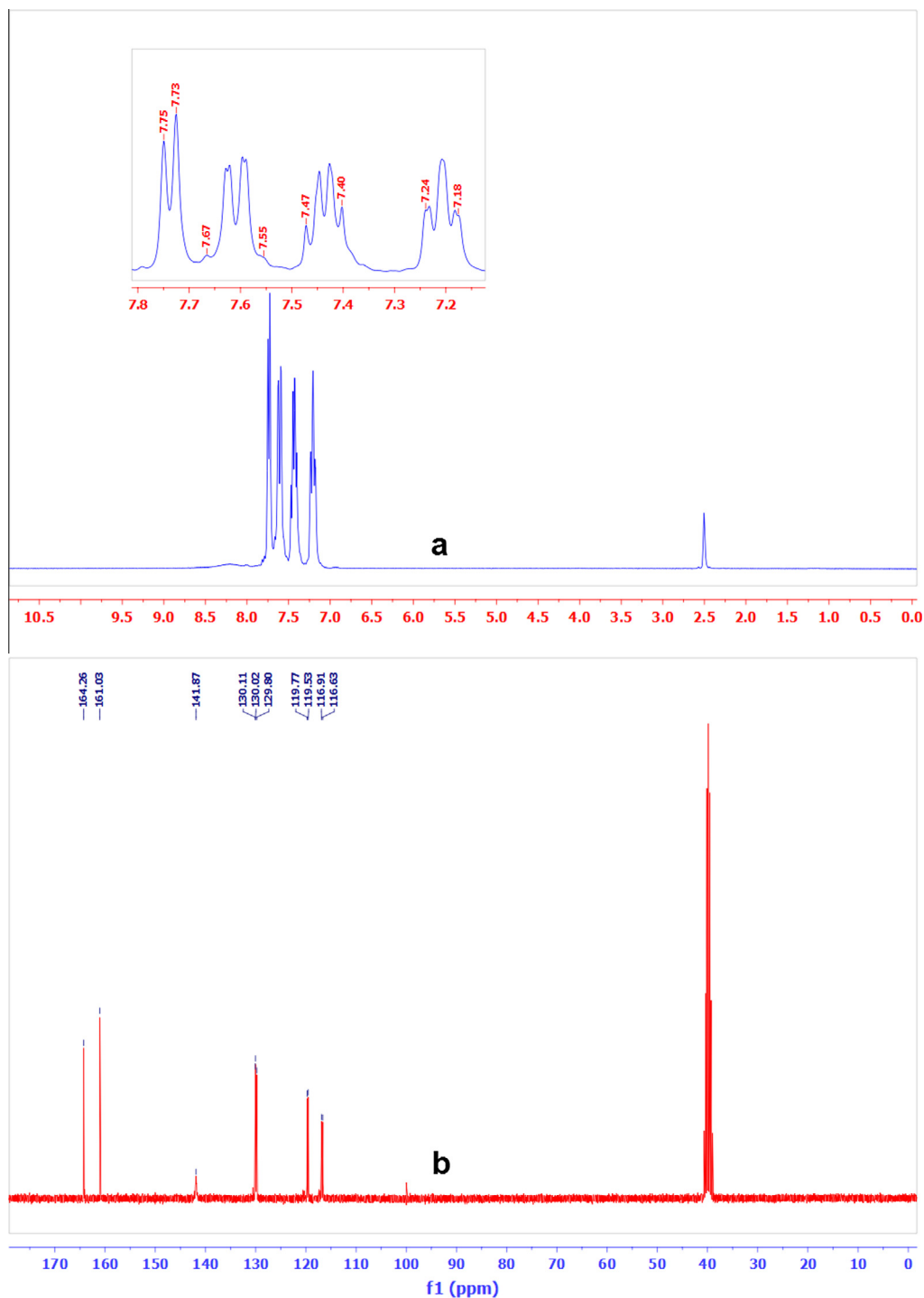


Fig. 6. (a) ^1H NMR (b) ^{13}C NMR spectra of 3FPBA in DMSO.

peaks at ca. 202 are not seen in the spectra. The wavelengths (λ), excitation energies (E), oscillator strengths (f), and calculated counterparts with major contributions can be seen in Table 5 both in ethanol and water solvents. The calculations also are replayed for the gas phase for monomer and dimer structures of the title molecule. The dimer results are doubled at ca. 248 nm. The last wavelength is increasing from monomer to dimer structure.

The frontier molecular orbitals (FMOs) play an important role in the electrical and optical properties. The HOMO and LUMO have the ability of electron giving and accepting characterizes, respectively. This is also used by the frontier electron density for

predicting the most reactive position in π -electron systems and also explains several types of reaction in conjugated system [58].

To determine the bonding scheme of 3FPBA compound, the frontier orbitals are pictured the surfaces. The energy gap is an important parameter in determining molecular electrical transport properties because it is a measure of electron conductivity, determined accordance of energy difference between HOMO and LUMO. The gap of energy was calculated at 5.75 eV for 3FPBA. The plots of MOs (HOMO and LUMO) and energy gap of HOMO–LUMO are given in Fig. S5. The important energy gaps of other FMOs of the title molecule were given in Table 6. The HOMO and LUMO orbitals

Table 4

The experimental and theoretical, ^1H and ^{13}C NMR isotropic chemical shifts (with respect to TMS) of 3FPBA with DFT (B3LYP/6-311++G(d,p)) method.

Atoms	Exp.	Monomer	Dimer
C(1)	129.80	131.01	137.90
C(2)	119.65	127.11	125.70
C(3)	162.64	174.13	171.65
C(4)	116.77	123.82	123.39
C(5)	141.87	134.94	134.84
C(6)	130.07	133.36	133.00
H(10)	–	4.19	5.19
H(11)	–	6.02	8.22
H(12)	7.18–7.24	7.24	7.45
H(13)	7.40–7.47	7.47	7.52
H(14)	7.55–7.67	7.61	7.65
H(15)	7.73–7.75	7.78	7.95

have nodes, placed as nearly symmetrically. The positive phase is red and the negative one is green. The charge density of the HOMO localized over ring of the molecule expect $\text{B}(\text{OH})_2$, but the LUMO is characterized by a charge distribution on all structure, expect H atoms (H_{10} and H_{11}). The energy gap explains the eventual charge transfer interactions taking place within the molecule. The HOMO and LUMO energy calculated by TD-DFT/B3LYP/6-311++G(d,p) method and the energy gap is following:

$$\text{HOMO}_{\text{energy}}(\text{B3LYP}) = -7.17 \text{ eV}$$

$$\text{LUMO}_{\text{energy}}(\text{B3LYP}) = -1.42 \text{ eV}$$

$$\text{HOMO} - \text{LUMO}_{\text{energy gap}}(\text{B3LYP}) = 5.75 \text{ eV}$$

Moreover the energy gaps of FMOs, between $\text{H}-1 \rightarrow \text{L}$, $\text{H} \rightarrow \text{L}$, $\text{H} \rightarrow \text{L}+2$ and $\text{H}-1 \rightarrow \text{L}+2$ orbital, are a critical parameter in determining molecular electrical transport properties. The energy gaps ($\text{H}-1 \rightarrow \text{L}$, $\text{H} \rightarrow \text{L}$, $\text{H} \rightarrow \text{L}+2$ and $\text{H}-1 \rightarrow \text{L}+2$) were calculated 6.09, 5.75, 6.57 and 6.91 eV for gas phase for the title molecule. These values were also calculated (monomer and dimer structures) in two solvents of the title molecule and presented in Table 6. Also the value of chemical hardness is 2.88 eV in gas phase, 2.89 eV in ethanol and water solvents for monomer structure. The chemical hardness is increasing 0.01 eV in solvents both monomer and dimer structures of the studied molecule. The other values of electronegativity, chemical potential and electrophilicity index are the same for two solvents for monomer and also dimer structures. The electronegativity value of gas phase is smaller than in ethanol and water solvents for monomer structure. But this value in gas phase is bigger than in ethanol and water solvent for dimer. The chemical potential showed reverse effect according to electronegativity. The values of electrophilicity index are the same for monomer as 3.21 eV. All values were gathered in Table 6 both monomer and dimer structures of TC conformer of the title molecule.

Total, partial, and overlap population density-of-states

The TDOS, PDOS, and OPDOS (or COOP (Crystal Orbital Overlap Population)) density of states [59,60], were calculated and created by convoluting the molecular orbital information with Gaussian curves of unit height and FWHM of 0.3 eV using the GaussSum 2.2 program [39] in point of the Mulliken population analysis. The COOP diagrams show the bonding, anti-bonding and nonbonding nature of the interaction of the two orbitals, atoms or groups. A positive and negative value indicate a bonding interaction and an anti-bonding interaction and zero value indicates nonbonding interactions, respectively [61] Additionally, the COOP diagrams allow us to the determination and comparison of the donor–acceptor properties of the ligands and ascertain the bonding, non-bonding.

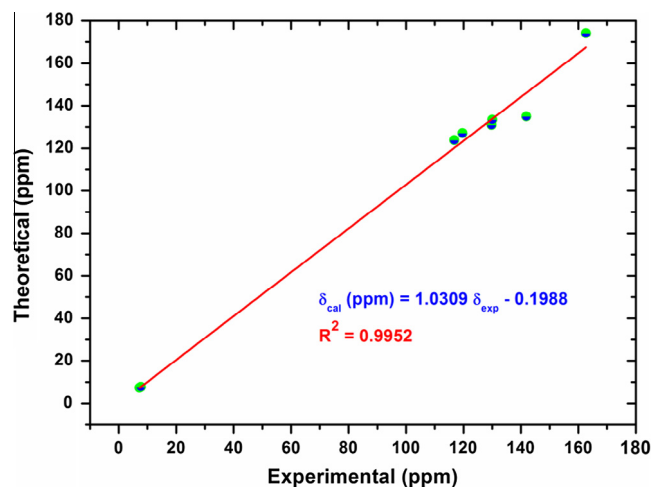


Fig. 7. Correlation graphic of the calculated and experimental (total) chemical shifts of 3FPBA.

A pictorial representation of molecular orbital (MO) compositions and their contributions to chemical bonding, the density of state of the molecule (TDOS, PDOS and COOP) were graphed and given in Figs. 9–11, respectively. In the boundary region, neighboring orbitals may show quasi degenerate energy levels. The PDOS mainly gives the composition of the fragment orbitals contributing to the molecular orbitals. The HOMO orbital are localized on phenyl ring and fluorine atom, their contributions are about 100%. The LUMO localized on the phenyl ring (89%), and $\text{B}(\text{OH})_2$ group (11%) of the title compound. To base the percentage shares of atomic orbitals or molecular fragments in the molecule is difficult to say bonding and anti-bonding properties. The COOP diagram and some of its orbitals of energy values of interaction between selected groups which are shown from figure easily, $\text{B}(\text{OH})_2$ group \leftrightarrow fluorine atom (blue line) system is near the zero (non-bonding interaction) as well as fluorophenyl \leftrightarrow $\text{B}(\text{OH})_2$ group systems (green line) and phenyl group \leftrightarrow fluorine atom (red line). As can be seen from the COOP plots for the headline compound have anti-bonding character in frontier HOMO and LUMO molecular orbitals for phenyl ring and fluorine atom. Also COOP showed bonding character from phenyl ring system to $\text{B}(\text{OH})_2$ group for HOMO orbital.

Molecular electrostatic potential surface

The MEPs simultaneously exhibits molecular size, shape as well as positive, negative and neutral electrostatic potential regions in terms of color grading and is very useful in research of molecular structure with its physicochemical property relationship. The MEPs generally show that the maximum positive region which preferred site for nucleophilic attack symptoms as blue color, while the maximum negative region which preferred site for electrophilic attack indications as red color. Because of the usefulness feature to study reactivity given that an approaching electrophile will be attracted to negative regions (where the electron distribution effect is dominant) [62,63].

To map onto the constant electron density surface, the MEPs of the studied molecule were plotted as 3D plots and 2D contour plots are illustrated in Fig. 12. The values of the electrostatic potential at the surface are illustrated by different colors (from red to blue) for different data (from the maximum negative to positive value) in the region with the MEPs. The potential rises from red to blue color. The colors line up between -0.06274 a.u. (dark red) and 0.06274 a.u. (dark blue) in the title compound. The strongest attraction and repulsion were represented blue and red color, respectively. The MEPs map of the title molecule showed that

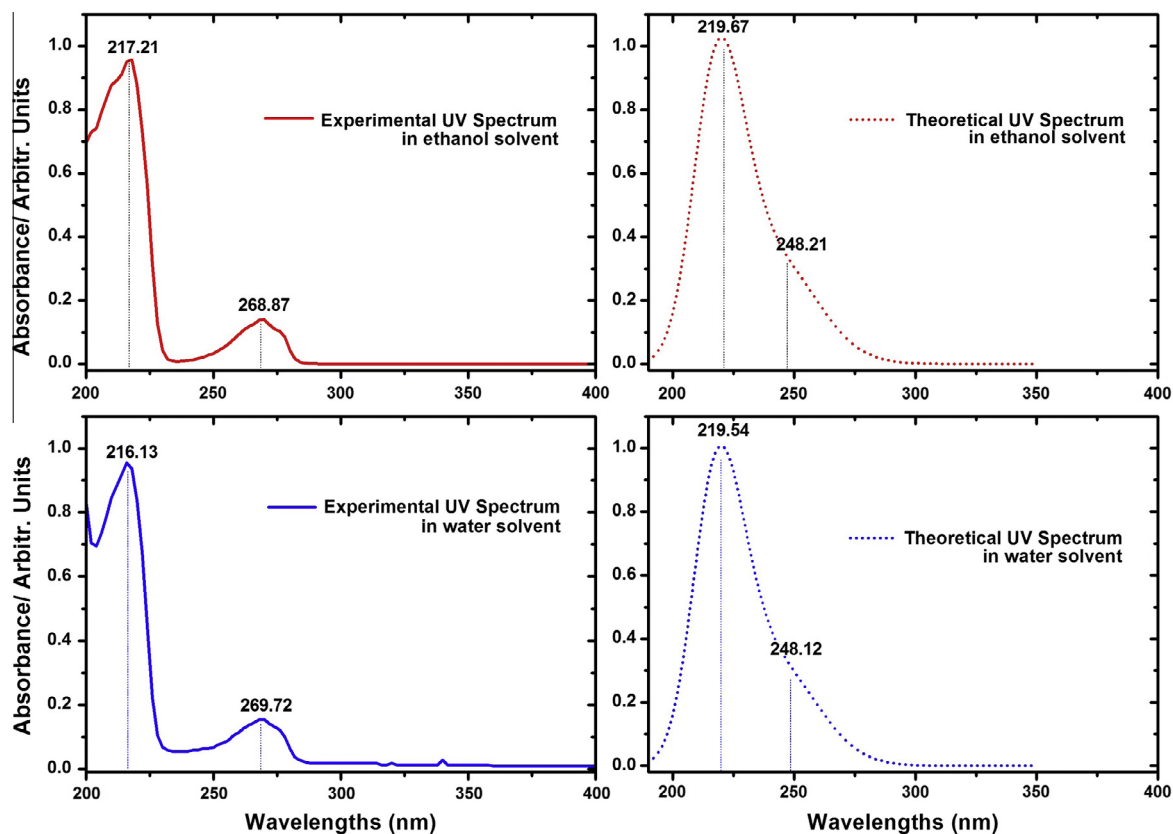


Fig. 8. The experimental and calculated UV-Vis spectra of 3FPBA in ethanol and water.

Table 5
The experimental and calculated wavelengths λ (nm), excitation energies (eV), oscillator strengths (f) of 3FPBA in ethanol, water solutions and gas phase for monomer and dimer structures of TC conformer.

TD-DFT/ B3LYP/6-311++G(d,p)					Experimental	
λ (nm)	E (eV)	f	Assignments	Major contributes	λ (nm)	E (eV)
<i>Monomer structure</i>						
Ethanol						
248.21	4.9957	0.0376	$\pi-\pi^*$	H-1 \rightarrow L+1 (18%), H \rightarrow L (76%)	268.87	4.6119
219.67	5.6449	0.1487	$\pi-\pi^*$	H-1 \rightarrow L (72%), H \rightarrow L+1 (20%)	217.21	5.7088
202.75	6.1160	0.0026	$\pi-\pi^*$	H \rightarrow L+2 (96%)	-	-
Water						
248.12	4.9976	0.0369	$\pi-\pi^*$	H-1 \rightarrow L+1 (18%), H \rightarrow L (76%)	269.72	4.6119
219.54	5.6483	0.1460	$\pi-\pi^*$	H-1 \rightarrow L (72%), H \rightarrow L+1 (20%)	216.13	5.7088
202.40	6.1264	0.0024	$\pi-\pi^*$	H \rightarrow L+2 (96%)	-	-
Gas phase						
248.54	4.98917	0.0257	$\pi-\pi^*$	H-1 \rightarrow L+1 (17%), H \rightarrow L (74%)	-	-
218.91	5.66436	0.0975	$\pi-\pi^*$	H-1 \rightarrow L (67%), H \rightarrow L+1 (24%)	-	-
212.52	5.83478	0.0054	$\pi-\pi^*$	H \rightarrow L+2 (88%)	-	-
<i>Dimer structure</i>						
Ethanol						
248.38	4.9924	0.0773	$\pi-\pi^*$	H-1 \rightarrow L+1 (36%), H \rightarrow L (41%)		
248.34	4.9932	0.0006	$\pi-\pi^*$	H-1 \rightarrow L (40%), H \rightarrow L+1 (35%)		
226.85	5.4662	0.0024	$\pi-\pi^*$	H-1 \rightarrow L+1 (50%), H \rightarrow L (49%)		
Water						
248.28	4.9943	0.0760	$\pi-\pi^*$	H-1 \rightarrow L+1 (35%), H \rightarrow L (41%)		
248.24	4.9952	0.0006	$\pi-\pi^*$	H-1 \rightarrow L (40%), H \rightarrow L+1 (35%)		
226.81	5.4671	0.0023	$\pi-\pi^*$	H-1 \rightarrow L+1 (50%), H \rightarrow L (49%)		
Gas phase						
248.69	4.9862	0.0526	$\pi-\pi^*$	H-1 \rightarrow L+1 (35%), H \rightarrow L (40%)		
248.67	4.9865	0.0004	$\pi-\pi^*$	H-1 \rightarrow L (40%), H \rightarrow L+1 (34%)		
227.94	5.4399	0.0011	$\pi-\pi^*$	H-1 \rightarrow L+1 (51%), H \rightarrow L (49%)		

Table 6

The calculated energy values and the energy gaps of 3FPBA molecule using by the TD-DFT/B3LYP method using 6-311++G(d,p) basis set for monomer and dimer structures of TC conformer.

Parameters	Monomer structure			Dimer structure		
	Gas	Ethanol	Water	Gas	Ethanol	Water
E_{total} (Hartree)	-507.6642397	-507.6728643	-507.6732822	-1015.343844	-1015.35763	-1015.358305
E_{HOMO} (eV)	-7.17	-7.19	-7.19	-7.21	-7.20	-7.20
E_{LUMO} (eV)	-1.42	-1.42	-1.42	-1.48	-1.44	-1.44
$E_{\text{HOMO}-1}$ (eV)	-7.51	-7.51	-7.51	-7.21	-7.20	-7.20
$E_{\text{LUMO}+1}$ (eV)	-0.66	-0.64	-0.64	-1.44	-1.41	-1.41
$E_{\text{LUMO}+2}$ (eV)	-0.60	-0.35	-0.34	-0.75	-0.65	-0.65
$E_{\text{HOMO}-1-\text{LUMOgap}}$ (eV)	6.09	6.09	6.09	5.73	5.76	5.76
$E_{\text{HOMO}-\text{LUMOgap}}$ (eV)	5.75	5.77	5.77	5.73	5.76	5.76
$E_{\text{HOMO}-\text{LUMO}+2\text{gap}}$ (eV)	6.57	6.84	6.85	6.46	6.55	6.55
$E_{\text{HOMO}-1-\text{LUMO}+2\text{gap}}$ (eV)	6.91	7.16	7.17	6.46	6.55	6.55
Chemical hardness (h)	2.88	2.89	2.89	2.87	2.88	2.88
Electronegativity (χ)	4.30	4.31	4.31	4.35	4.32	4.32
Chemical potential (μ)	-4.30	-4.31	-4.31	-4.35	-4.32	-4.32
Electrophilicity index (ω)	3.21	3.21	3.21	3.29	3.24	3.24

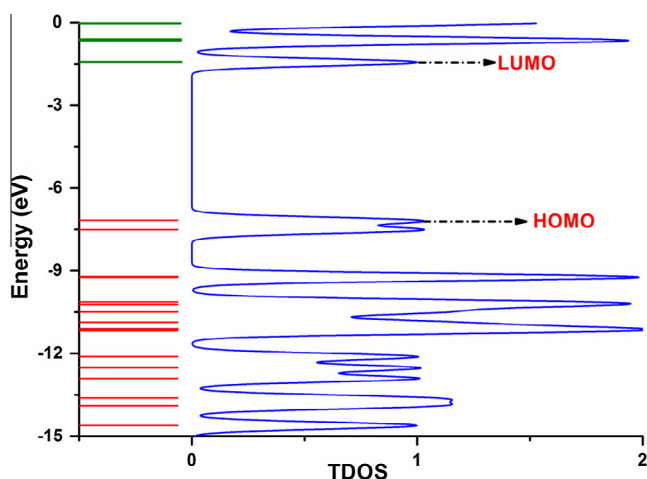


Fig. 9. The total electronic density of states diagram of 3FPBA.

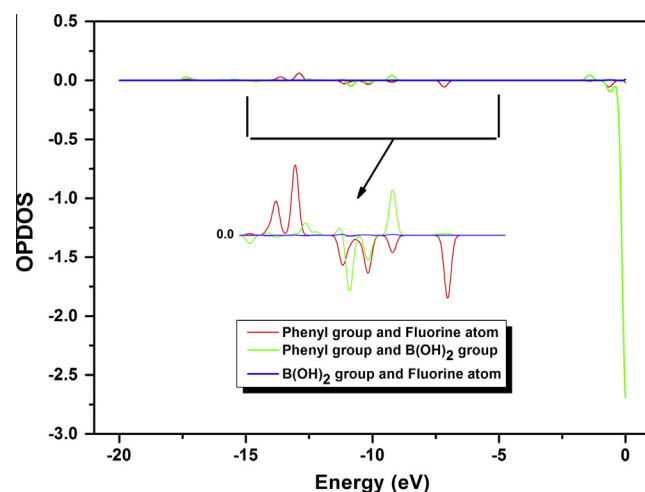


Fig. 11. The overlap population electronic density of states diagram of 3FPBA.

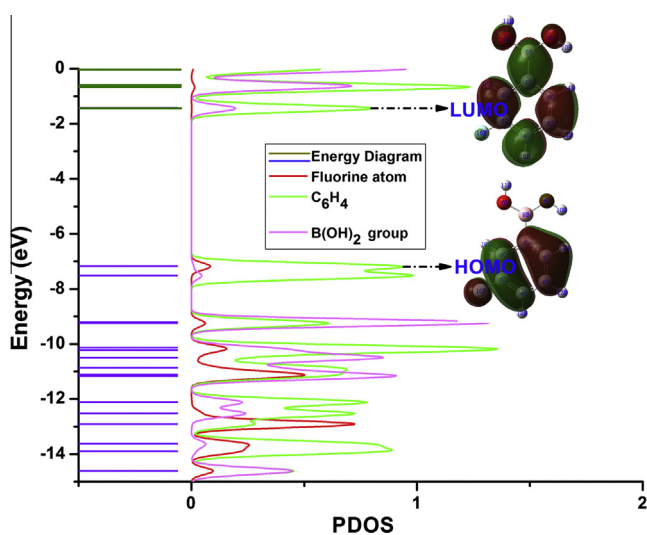


Fig. 10. The partial electronic density of states diagram of 3FPBA.

while regions having the positive potential are near hydrogen atom (except H_{12}), the regions having the negative potential are over oxygen and fluorine atoms. From these results, we can say that

hydrogen (especially H_{11} and H_{10}) atoms indicate the strongest attraction and oxygen and fluorine atoms indicate the strongest repulsion (see Fig. 12). The sliced 2D contour map of MEPs of the title molecule provides more exhaustive information regarding MEP distribution, by showing the values in an assortment of spatial site around the molecule. The 2D MEPs were drawn in the molecular plane of the studied molecule. The around of oxygen atoms have electron rich region and the around of hydrogen atoms corresponds to the electron deficient region. The maximum values of negative and positive potential corresponding to the nucleophilic and electrophilic region are 0.04 a.u. and 0.8 a.u., respectively.

Mulliken atomic charges

The reactive atomic charges play an important role in the application of quantum mechanical calculations in the molecular system. The Mulliken atomic charges were calculated based on by using DFT/B3LYP method 6-311++G(d,p) basis set. The Mulliken atomic charges of 2,3-DFPBA [27], phenyl boronic acid (PBA) and monomer and dimer structures of 3FPBA molecule are tabulated in Table 7. The Mulliken atomic charges of these molecules and the studied molecule (monomer) are illustrated in Fig. 13. The results show that substitution of the aromatic ring by fluorine atom leads to a redistribution of electron density [27]. Namely, the charge of $B(OH)_2$ group is the same distribution (negative or positive) in both molecules, however, ring of molecules exhibit a

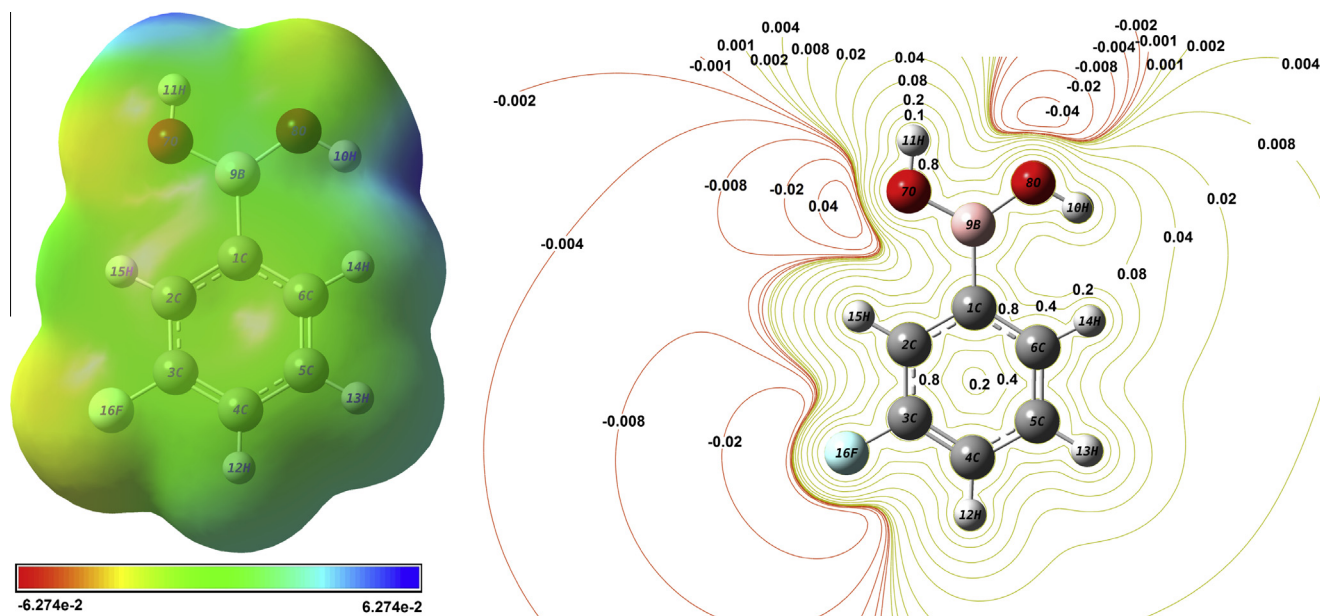


Fig. 12. Molecular electrostatic potential surface 3D map and 2D contour map for 3FPBA.

different charge with each other. For example, the charge of C₁ is negative value for PBA and 3FPBA but it is positive for 2,3-DFPBA molecule [27], this can be the effect of the fluorine atom near C1 atom. The same interactions showed for the charges of C2 and C6 atoms as effected the OH groups for PBA and 3FPBA molecules. Hydrogen atoms exhibit a positive charge, which is an acceptor atom for all molecules. The Mulliken atomic charges of monomer and dimer structures of 3FPBA molecule are showed the same distributions nearly parallel values except oxygen atoms (O₇ and O₈) and H₁₁ atom. Also the Mulliken atomic charges of the title molecule were showed the same charges but fluorine atom was different (mode number 16) charge, instead of hydrogen atom.

Thermodynamic features

The global minimum energy obtained for the title structure optimization of B3LYP with 6-311++G(d,p) basis set is

Table 7

Comparison of Mulliken charges of 3-fluorophenylboronic acid (monomer and dimer) with phenylboronic acid and 2,3-difluorophenyl boronic acid using by B3LYP/6-311++G(d,p) basis set.

Atoms	PBA	3-FPBA		2,3-DFPBA ^a
	Monomer	Monomer	Dimer	Monomer
C1	-0.680	-0.751	-0.641	0.080
C2	0.188	0.600	0.485	-0.193
C3	-0.440	-0.857	-0.857	-0.257
C4	-0.022	0.439	0.473	0.343
C5	-0.352	-0.438	-0.427	-0.364
C6	0.207	0.135	0.148	-0.171
O7	-0.376	-0.369	-0.576	-0.393
O8	-0.366	-0.369	-0.561	-0.378
B9	0.531	0.531	0.614	0.590
H10	0.230	0.235	0.277	0.251
H11	0.288	0.289	0.510	0.293
H12	0.161	0.201	0.200	0.209
H13	0.161	0.170	0.173	0.177
H14	0.114	0.121	0.117	0.200
F15/H15	0.196	0.234	0.233	-0.206
F16/H16	0.161	-0.170	-0.168	-0.181

^a The X-ray data from Ref. [27].

-507.6642397 a.u. The zero-point vibrational energy (ZPVEs), thermal energy, specific heat capacity, rotational constants, entropy and dipole moment of monomer conformers of the studied molecule for C₁ and C_s symmetry point groups, by DFT/B3LYP/6-311++G(d,p) method at room temperature in the ground state are listed in Table S2.

The statically thermodynamic functions: heat capacity (C), entropy (S), and enthalpy changes (ΔH) for the present molecule were obtained from the theoretical harmonic frequencies and listed in Table S3 according to vibrational analysis. These thermodynamic functions are increasing with temperature ranging from 100 to 700 K, due to the fact that the molecular vibrational intensities increase with temperature. The correlation equations between heat capacity, entropy, enthalpy changes and temperatures are fitted by quadratic formulas and the corresponding fitting factors (R²) for these thermodynamic properties. The relations between these thermodynamic properties and temperature are represented in Fig. S6. R² values are 0.9994, 0.9999 and 0.9998, respectively. The corresponding fitting equations are as follows:

$$C = -0.72294 + 0.13485T - 6.6605 \times 10^{-5}T^2 \quad (R^2 = 0.9994)$$

$$S = 54.56467 + 0.14138T - 3.6964 \times 10^{-5}T^2 \quad (R^2 = 0.9999)$$

$$\Delta H = -0.469021 + 0.00996T + 4.1552 \times 10^{-5}T^2 \quad (R^2 = 0.9998)$$

As a result the thermodynamical data supply helpful information for the further study on 3FPBA. These results also showed good coherence with the previous work for the similar compounds [27]. They can be used to calculate the other thermodynamic energies according to relationships of thermodynamic functions and estimate directions of chemical reactions according to the second law of thermodynamics in Thermochemical field. Notice: all thermodynamic calculations were done in gas phase and they could not be used in solution.

Nonlinear optical properties and dipole moment

The electronic dipole moment (μ), molecular polarizability, anisotropy of polarizability and molecular first hyperpolarizability

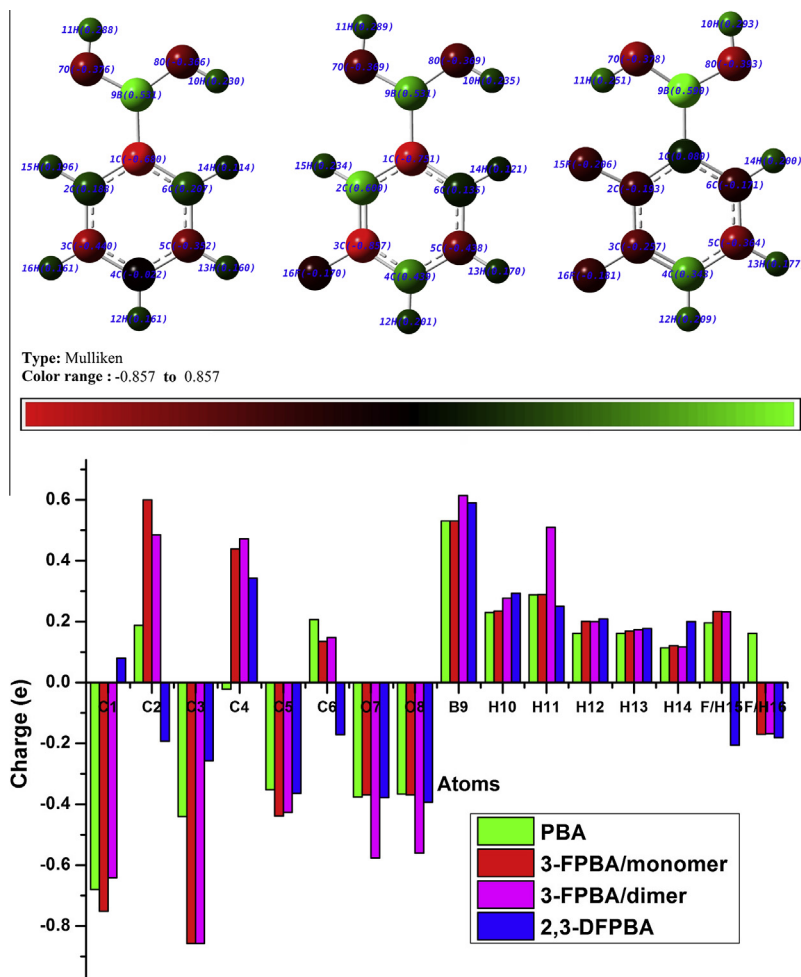


Fig. 13. The Mulliken charge distribution for PBA, 3FPBA and 23DFPBA molecules.

of 3FPBA molecule are investigated in this work. We used a frequency job output file of Gaussian to obtain the polarizability (α) and hyperpolarizability (β) tensors. However, the units of α and β values of Gaussian output are in atomic units (a.u.) so they were converted into electronic units (esu) (for α ; 1 a.u. = 0.1482×10^{-24} esu, for β ; 1 a.u. = 8.6393×10^{-33} esu). The calculated parameters (α , β and μ) for the title compound are gathered and listed in Table S4.

It is well known that the higher values of dipole moment, molecular polarizability, and hyperpolarizability are important for more active NLO properties. The calculated value of dipole moment was found to be 2.7815 Debye. The highest value of dipole moment is observed for component μ_y . In this direction, this value is equal to 2.5809 D and μ_z is the smallest one. The calculated values of polarizability and anisotropy of the polarizability of the title molecule are $13.056968 \times 10^{-24}$ esu and $29.28633309 \times 10^{-24}$ esu, respectively. The magnitude of the molecular hyperpolarizability β is one of important key factors in a NLO system. The calculated first hyperpolarizability value (β) of 3FPBA is equal to $2330.839482 \times 10^{-33}$ esu. If we compare the common values of urea; the first hyperpolarizability, polarizability, anisotropy of the polarizability and dipole moment values of 3FPBA are larger than those of urea.

Conclusions

The molecular parameters, frequency assignments, electronic transition and magnetic properties of 3FPBA molecule were performed by using FT-IR, FT-Raman, ^1H and ^{13}C NMR and UV-Vis

techniques both experimentally and theoretically. The theoretical computations were studied both monomer and dimer structures. The most stable conformer was identified. The experimental information on the structural parameters available in the literature, the optimized geometric parameters (bond lengths and bond angles) were theoretically determined by B3LYP/6-311++G(d,p) level of theory and compared with the X-ray results and similar structures. The vibrational FT-IR and FT-Raman spectra of 3FPBA were recorded. The magnetic properties of the molecule were observed and calculated. The chemical shifts were compared with the experimental data in DMSO solution, showing a very good agreement both for ^1H and ^{13}C . The electronic properties were also calculated and the experimental electronic spectra were recorded with help of UV-Vis spectrometer. The molecular orbitals, MEPs contour/surface were drawn and the electronic transitions were identified for UV-Vis spectra may lead to the understanding of properties and dynamics of the molecule. The correlations between the statistical thermodynamics and temperature were obtained. It is seen that the heat capacities, entropies and enthalpies increase with the increasing temperature owing to the intensities of the molecular vibrations increase with increasing temperature. The comparison of predicted bands with experimental was done and shows an acceptable general agreement.

Acknowledgement

This work was supported by the Celal Bayar University Research fund through research Grant No.: FBE-2011/70.

Appendix A. Supplementary material

Supplementary data associated with this article can be found in the online version, at <http://dx.doi.org/10.1016/j.saa.2014.08.141>.

References

- [1] E. Frankland, B.F. Duppa, *Justus Liebigs Ann. der Chem.* 115 (3) (1860) 319–322.
- [2] N.A. Petasis, *Aust. J. Chem.* 60 (2007) 780–795.
- [3] P.C. Trippier, C. McGuigan, *Med. Chem. Commun.* 1 (2010) 183–198.
- [4] E. Cuthbertson, *Boronic Acids: Properties and Applications*, Alfa Aesar, Heysham, 2006.
- [5] D.G. Hall (Ed.), *In Boronic Acids*, first ed., Wiley-VCH, Weinheim, 2005.
- [6] S.J. Rettig, J. Trotter, *Can. J. Chem.* 55 (1977) 3071–3075.
- [7] J.A. Faniran, H.F. Shurvell, *Can. J. Chem.* 46 (1968) 2089–2095.
- [8] M.K. Cyrański, A. Jezierska, P. Klimentowska, J.J. Panek, A. Sporzynski, *J. Phys. Org. Chem.* 21 (2008) 472–482.
- [9] Y.M. Wu, C.C. Dong, S. Liu, H.-J. Zhu, Y.-Z. Wu, *Acta Cryst. E* 62 (2006) o4236–o4237.
- [10] M.R. Shimpi, N. Seetha Lekshmi, V.R. Pediretti, *Cryst. Growth Des.* 7 (10) (2007) 1958–1963.
- [11] P. Rodriguez-Cuamatzi, H. Tlahuext, H. Höpfl, *Acta Cryst. E* 65 (2009) o44–o45. E65.
- [12] B. Zarychta, J. Zaleski, A. Sporzynski, M. Dabrowski, J. Serwatowski, *Acta Cryst. C* 60 (2004) o344–o345.
- [13] A. Vega, M. Zarate, H. Tlahuext, H. Höpfl, *Acta Cryst. E* 66 (2010) o1260.
- [14] M. Karabacak, E. Kose, A. Atac, A.M. Asiri, M. Kurt, *J. Mol. Struct.* 1058 (2014) 79–96.
- [15] M. Karabacak, E. Kose, A. Atac, E.B. Sas, A.M. Asiri, M. Kurt, *J. Mol. Struct.* (2014), in press.
- [16] N.C. Handy, C.W. Murray, R.D. Amos, *J. Phys. Chem.* 97 (1993) 4392–4396.
- [17] P.J. Stephens, F.J. Devlin, C.F. Chabalowski, M.J. Frisch, *J. Phys. Chem.* 98 (1994) 11623–11627.
- [18] F.J. Devlin, J.W. Finley, P.J. Stephens, M.J. Frisch, *J. Phys. Chem.* 99 (1995) 16883–16902.
- [19] S.Y. Lee, B.H. Boo, *Bull. Korean Chem. Soc.* 17 (1996) 760–764.
- [20] G. Rauhut, P. Pulay, *J. Phys. Chem.* 99 (1995) 3093–3100.
- [21] M. Kurt, *J. Raman Spectrosc.* 40 (2009) 67–75.
- [22] M. Kurt, T.R. Sertbakan, M. Özduran, M. Karabacak, *J. Mol. Struct.* 921 (2009) 178–187.
- [23] Ö. Alver, *Chimie* 14 (2011) 446–455.
- [24] Ö. Alver, C. Parlak, *Vib. Spectr.* 54 (2010) 1–9.
- [25] M. Kurt, T.R. Sertbakan, M. Özduran, *Spectrochim. Acta A* 70 (2008) 664–673.
- [26] A.K. Sachan, S.K. Pathak, L. Sinha, O. Prasad, M. Karabacak, A.M. Asiri, *J. Mol. Struct.* (2014), in press.
- [27] M. Karabacak, E. Kose, A. Atac, M.A. Cipiloglu, M. Kurt, *Spectrochim. Acta A* 97 (2012) 892–908.
- [28] M. Karabacak, L. Sinha, O. Prasad, A.M. Asiri, M. Cinar, *Spectrochim. Acta A* 115 (2013) 753–766.
- [29] U. Rani, M. Karabacak, O. Tanrıverdi, M. Kurt, N. Sundaraganesan, *Spectrochim. Acta A* 92 (2012) 67–77.
- [30] P. Hohenberg, W. Kohn, *Phys. Rev.* 136 (1964) B864–B871.
- [31] A.D. Becke, *J. Chem. Phys.* 98 (1993) 1372.
- [32] C. Lee, W. Yang, R.G. Parr, *Phys. Rev. B* 37 (1988) 785–789.
- [33] M.J. Frisch et al. GAUSSIAN 09, Revision A.1, Gaussian Inc., Wallingford, CT, 2009.
- [34] N. Sundaraganesan, S. Ilakiamani, H. Salem, P.M. Wojciechowski, D. Michalska, *Spectrochim. Acta A* 61 (2005) 2995–3001.
- [35] M. Kurt, P.C. Babu, N. Sundaraganesan, M. Cinar, M. Karabacak, *Spectrochim. Acta A* 79 (2011) 1162–1170.
- [36] J. Baker, A.A. Jarzecki, P. Pulay, *J. Phys. Chem. A* 102 (1998) 1412–1424.
- [37] P. Pulay, J. Baker, K. Wolinski, Green Acres Road, Suite A, Fayetteville, AR 72703, USA, 2013.
- [38] K. Wolinski, J.F. Hinton, P. Pulay, *J. Am. Chem. Soc.* 112 (1990) 8251–8260.
- [39] N.M. O’Boyle, A.L. Tenderholt, K.M. Langner, *J. Compd. Chem.* 29 (2008) 839–845.
- [40] A.R. Choudhury, T.N. Guru Row, *Acta Crystallogr. E* 60 (2004) o1595.
- [41] M. Karabacak, E. Kose, M. Kurt, *J. Raman Spectrosc.* 41 (2010) 1085–1097.
- [42] M. Karabacak, L. Sinha, O. Prasad, Z. Cinar, M. Cinar, *Spectrochim. Acta A* 93 (2012) 33–46.
- [43] G. Kahraman, O. Beskarcler, Z.M. Rzaev, E. Piskin, *Polymer* 45 (2004) 5813–5828.
- [44] G. Vargas, I. Hernandez, H. Höpfl, M. Ochoa, D. Castillo, N. Farfan, R. Santillan, E. Gomez, *Inorg. Chem.* 43 (2004) 8490–8500.
- [45] Y. Erdogdu, M.T. Gulluoglu, M. Kurt, *J. Raman Spectrosc.* 40 (2009) 1615–1623.
- [46] M. Silverstein, G. Clayton Basseler, C. Morill, *Spectrometric Identification of Organic Compounds*, Wiley, New York, 2001.
- [47] G. Varsanyi, *Assignments of Vibrational Spectra of Seven Hundred Benzene Derivatives*, Springer, 1974, vol. 1–2.
- [48] R.A.R. Pearce, D. Steele, K.J. Radcliffe, *J. Mol. Struct.* 15 (1973) 409–414.
- [49] N.A. Narasimham, M.Z. El-Saban, J. Rud-Nielson, *J. Chem. Phys.* 24 (1956) 420–433.
- [50] C.N.R. Rao, *Chemical Applications of Infrared Spectroscopy*, Academic Press, New York, 1963.
- [51] T. Schlick, *Molecular Modeling and Simulation: An Interdisciplinary Guide*, second ed., Springer, New York, 2010.
- [52] A. Atac, M. Karabacak, C. Karaca, E. Kose, *Spectrochim. Acta A* 85 (2012) 145–154.
- [53] N. Subramania, N. Sundaraganesan, J. Jayabharathi, *Spectrochim. Acta A* 76 (2010) 259–269.
- [54] H.O. Kalinowski, S. Berger, S. Braun, *Carbon-13 NMR Spectroscopy*, John Wiley & Sons, Chichester, 1988.
- [55] K. Pihlaja, E. Kleinpeter (Eds.), *Carbon-13 Chemical Shifts in Structural and Stereochemical Analysis*, VCH Publishers, Deerfield Beach, 1994.
- [56] D. Guillaumont, S. Nakamura, *Dyes Pigments* 46 (2000) 85–92.
- [57] J. Fabian, *Dyes Pigments* 84 (2010) 36–53.
- [58] K. Fukui, T. Yonezawa, H. Shingu, *J. Chem. Phys.* 20 (1952) 722–725.
- [59] R. Hoffmann, *Solids and Surfaces: A Chemist’s View of Bonding in Extended Structures*, VCH Publishers, New York, 1988.
- [60] J.G. Malecki, *Polyhedron* 29 (2010) 1973–1979.
- [61] M. Chen, U.V. Waghmare, C.M. Friend, E. Kaxiras, *J. Chem. Phys.* 109 (1998) 6680–6854.
- [62] J.S. Murray, K. Sen, *Molecular Electrostatic Potentials, Concepts and Applications*, Elsevier, Amsterdam, 1996.
- [63] E. Scrocco, J. Tomasi, in: P. Lowdin (Ed.), *Advances in Quantum Chemistry*, Academic Press, New York, 1978.